



TRIUMF Beam Physics Note  
TRI-BN-16-CR-SIM  
Oct.10, 2016

# Improved Simulation for Centre Region of TRIUMF 500 MeV Cyclotron

*Y.-N. Rao*

*TRIUMF*

**Abstract:** This note summarizes the results of simulation we improved for the centre region of TRIUMF 500 MeV cyclotron using TRIWHEEL.

# 1 Objective

The TRIUMF 500 MeV cyclotron delivered routinely a total current up to  $200 \mu\text{A}$  protons for 15 years till 2001. Since 2002, developments towards  $300 \mu\text{A}$  total extraction became compelling because of the ISAC expansion. To meet future requirements (for addition of BL4N), a total extraction of  $310 - 450 \mu\text{A}$  shall be envisioned. With such an increase of beam current, the space charge effect becomes a major concern in the centre region, as it limits the maximum amount of beam current achievable out of the machine. Therefore, numerical simulation [1] on beam orbits with the space charge force has begun, starting from the injection gap. In order to benchmark the simulations performed prior to the collective effect inclusion, we resurrected TRIWHEEL and improved it to allow adopting the standard magnetic field map (“policyinita6.dat”) for the simulations. In 1970s, TRIWHEEL was specifically employed in the centre region modeling and single particle orbit dynamics studies for the TRIUMF cyclotron [2] [3]. It integrates numerically by Runge-Kutta method the 3-D equations of motion of charged particles under the action of 3-D rf electric field and static magnetic field, using time as the independent variable. This note summarizes the results of simulation that we refined.

## 2 3-D Electric Field

TRIWHEEL works in a Cartesian frame, using time instead of azimuth as the independent variable. For TRIUMF cyclotron, the Cartesian frame is defined such that the origin is in the machine centre,  $+x$  axis is along the dee gap centre-line pointing to the right (i.e. to the injection gap side),  $+y$  axis is perpendicular to the dee gap,  $x$ - $o$ - $y$  is on the geometric median plane of the cyclotron, and  $+z$  axis is axially upward. The  $x$ - $y$ - $z$  is right-handed.

The electric field was calculated from a 3-dimensional arrays of the electric potentials, produced with relaxation code RELAX3D [4], normalized to the dee voltage amplitude. Limited by the computer memory, in the history the whole centre region geometry was split into left and right two parts for the RELAX3D computation, which was then combined, with a rectangular box filled up in between (see Fig.1). This box represents a dead region near the centre of the centre post. Such a simplified model worked fine in terms of the potential distribution, as the electric field has already dropped to zero at everywhere outside the box in  $y$  direction. But in fact, this is an incomplete model of the electrode geometries. We want to make the centre region model complete because this is important when we need to locate where the particles get lost exactly around the centre post. Therefore, we strived to improve the model so that it now reflects the geometries more realistically. This is shown in Fig.2.

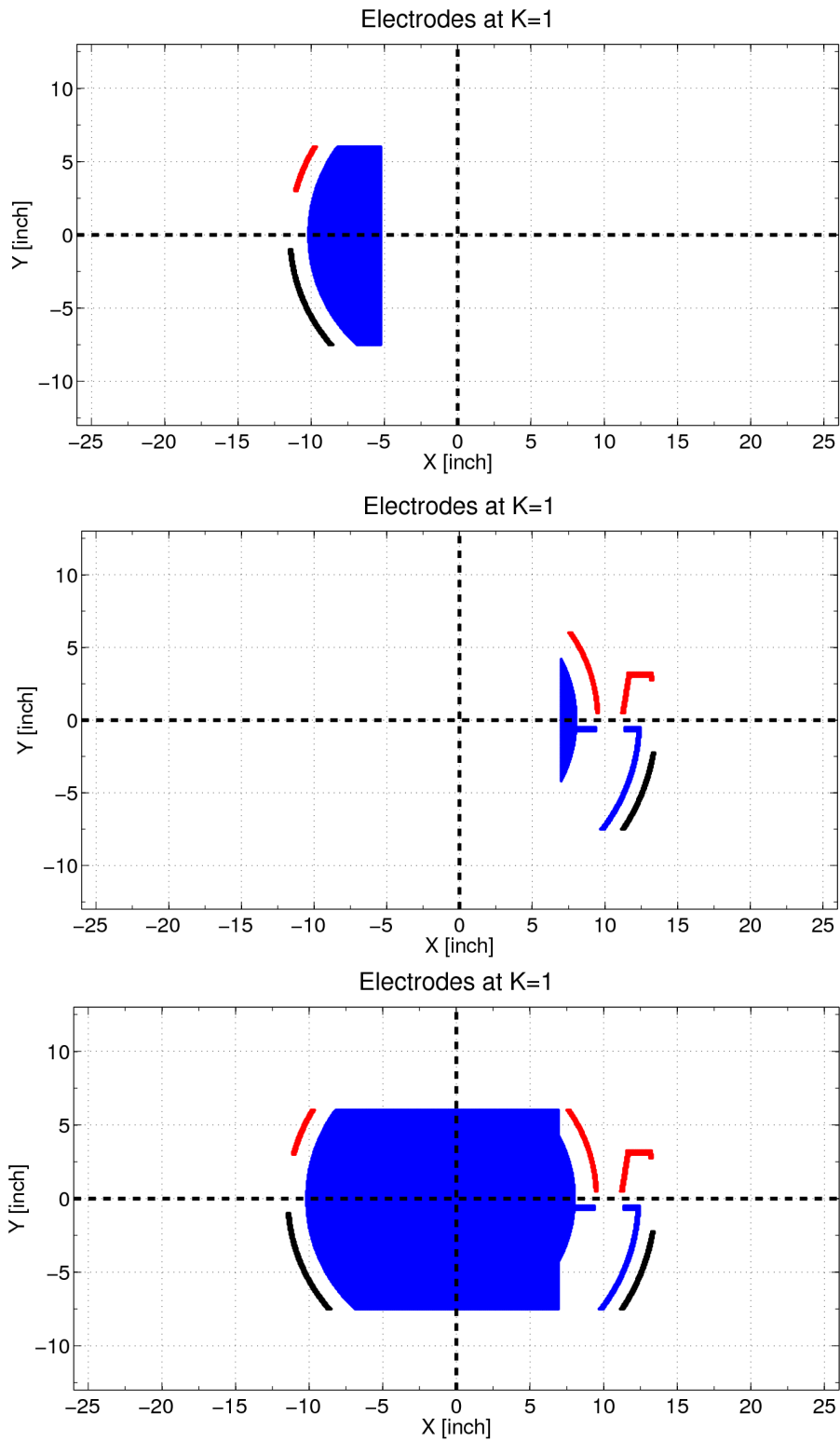


Figure 1: *Historically, the TRIUMF centre region geometry was split into left (Top) and right (Middle) two parts for the relaxation computation, and then combined with a rectangular box filled up in between (Bottom). All these are shown in the geometrical median plane (GMP).*

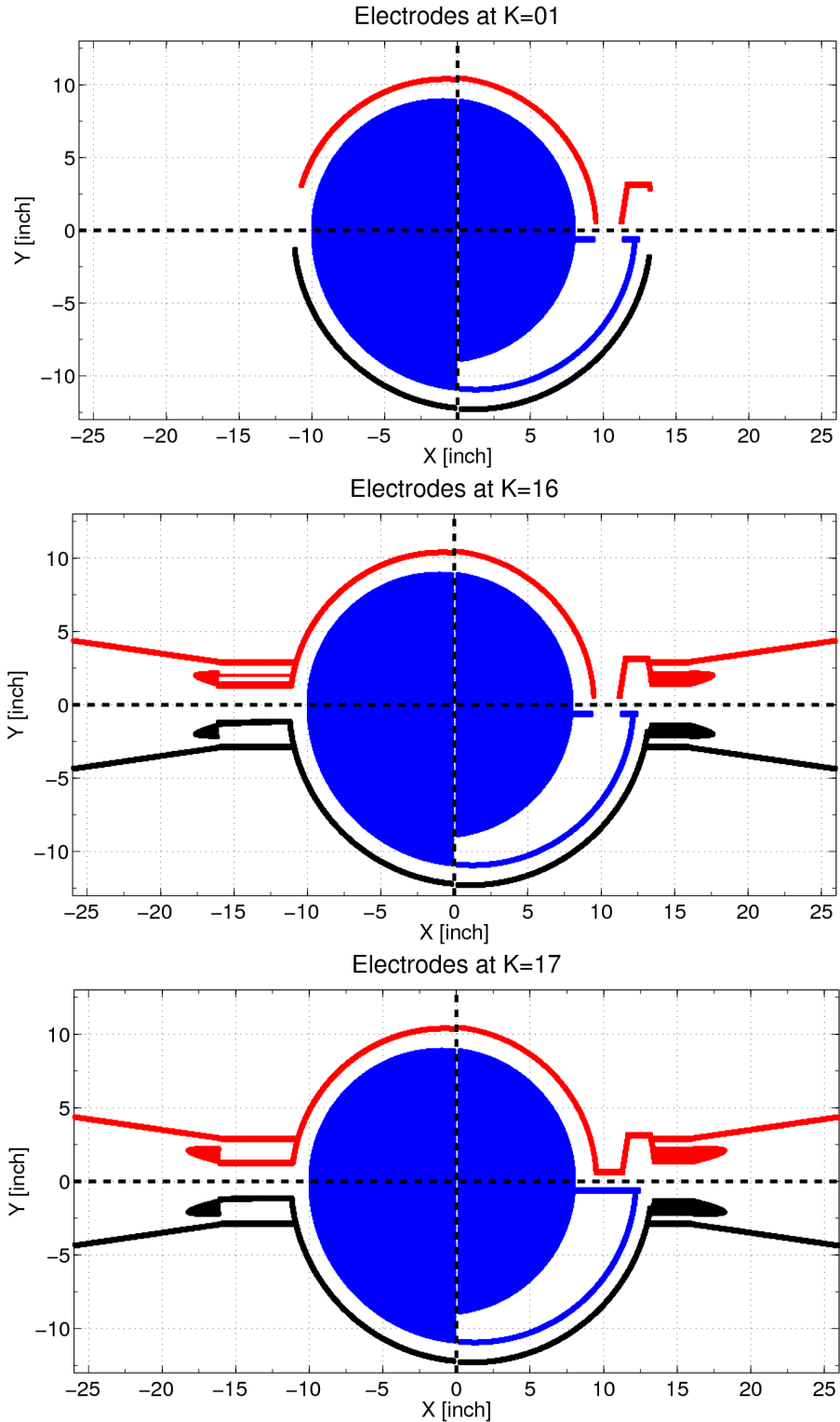


Figure 2: Improved model of the centre region geometry, shown as an example in 3 different planes vertically: GMP (Top),  $k=16$  (Middle) and  $k=17$  (Bottom). The vertical grid step size is 0.0625". These realistically reflect the electrode's geometries. Note that the blue marks ground potential, the red marks positive potential +1 while the black marks negative potential -1 which are normalized to the dee voltage amplitude.

### 3 Comparison with CYCLONE

Firstly, as a cross-check for orbit calculation using the remodeled 3-D electric field map, we ran TRIWHEEL and CYCLONE [5] respectively to track a single particle through the centre region, starting from the injection gap. For both runs, the particle's initial coordinate remained exactly the same. The results are shown in Fig.3–Fig.8 for a comparison about the orbit in the  $(x, y)$  plane, the rf phase angle, energy,  $(z, p_z)$  and  $(r, p_r)$  vs. turn.

Apparently, they are perfectly agreed. This gives us confidence in the orbit calculations with these codes. Should be noted that TRIWHEEL and CYCLONE are different in many ways, for example, TRIWHEEL integrates equations of motion in the Cartesian frame using time as independent variable, while CYCLONE works in the polar frame using azimuth as independent variable.

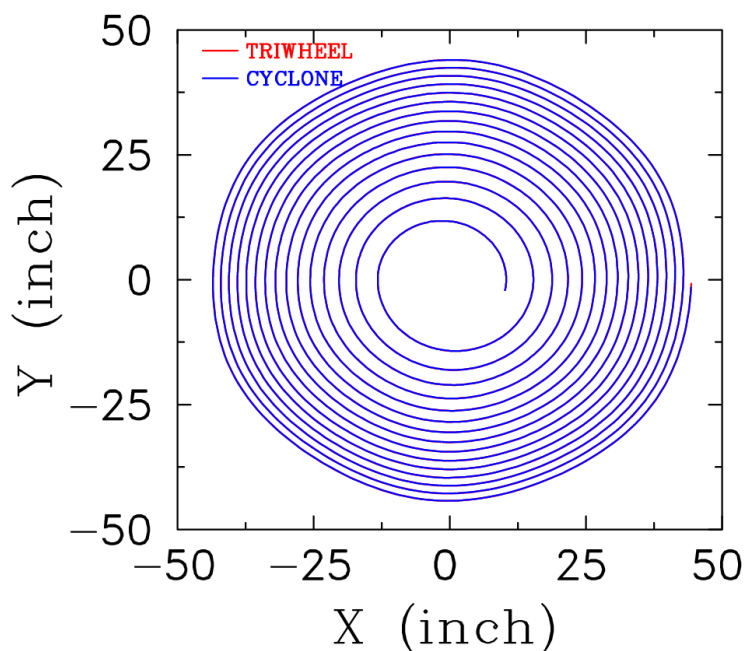


Figure 3: Comparison of single particle's orbit in  $(x, y)$  plane between the TRIWHEEL run and CYCLONE run. For the sake of clearness, here only 15 turns are plotted. They are very much overlapped and are perfectly agreed.

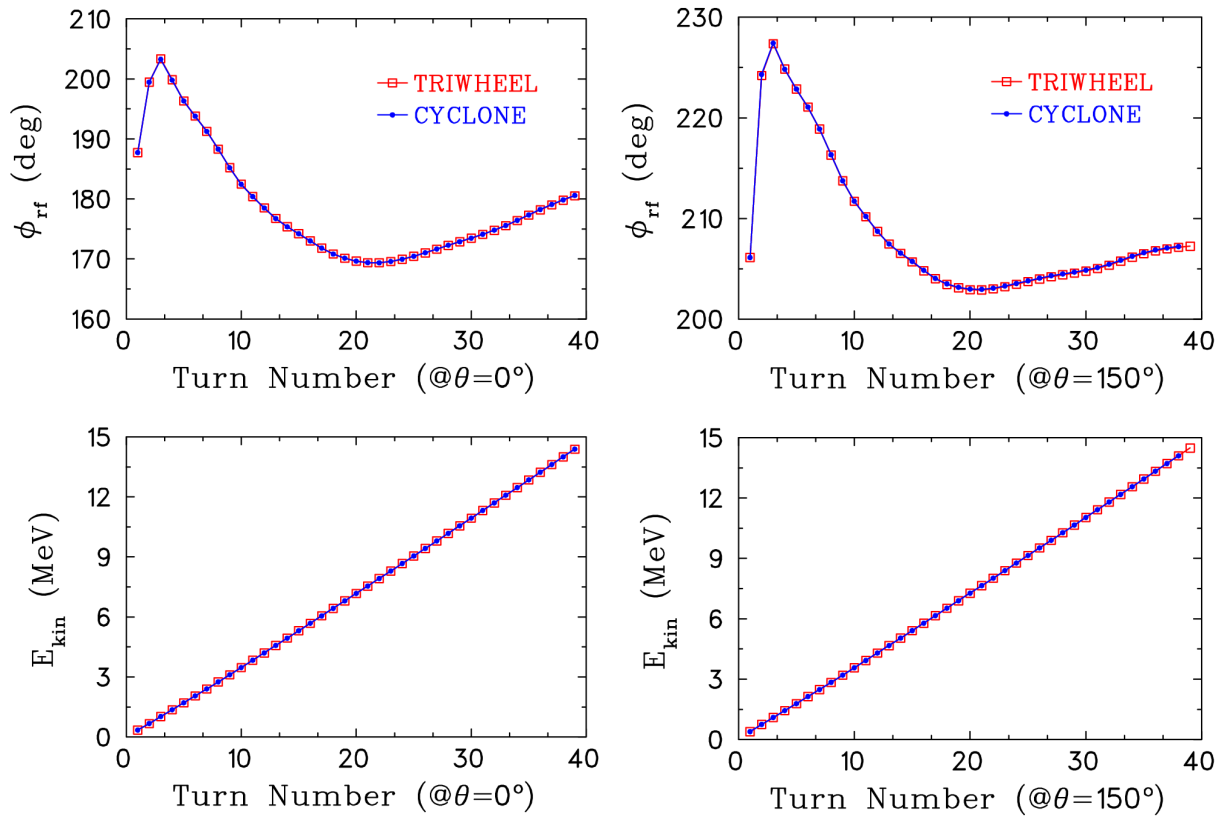


Figure 4: Comparison of single particle's rf phase and energy recorded at azimuths of e.g.  $0^\circ$  and  $150^\circ$  respectively, between the TRIWHEEL run and CYCLONE run.

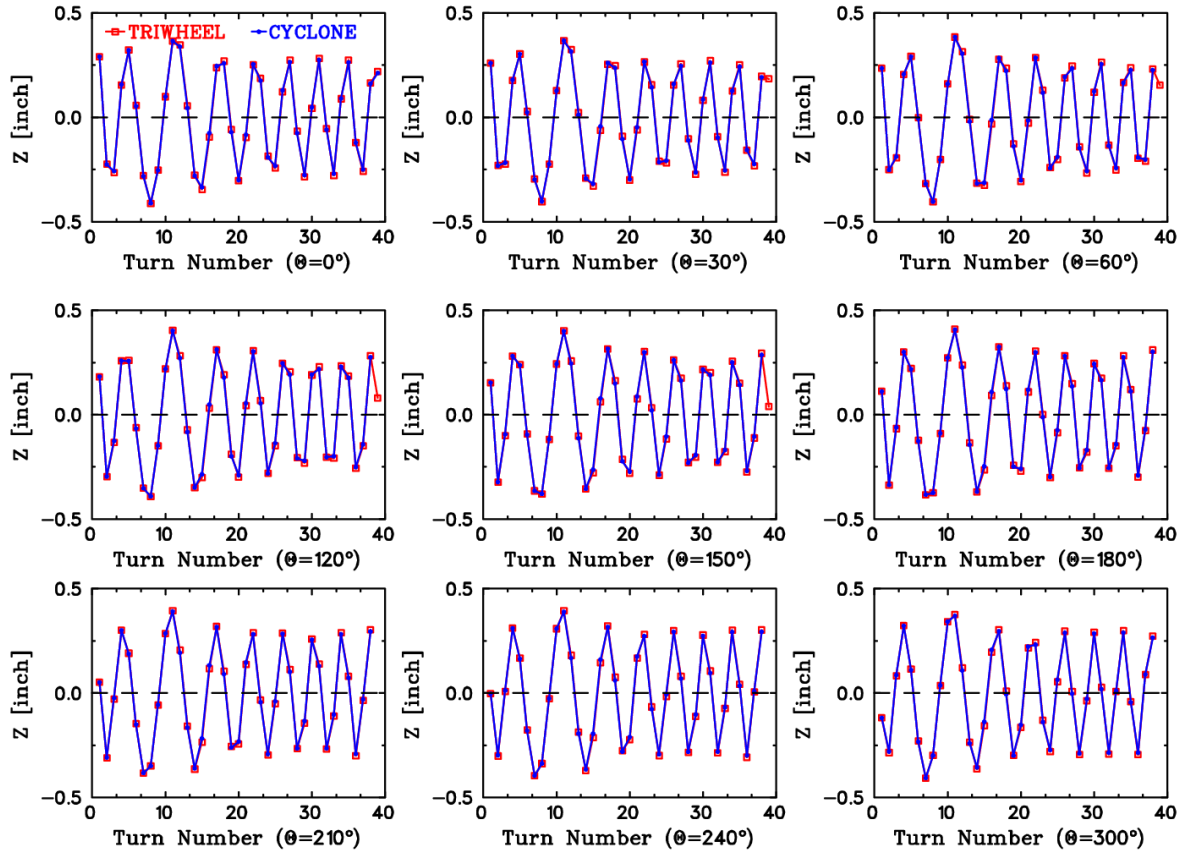


Figure 5: Comparison of single particle's axial coordinate  $z$  recorded at various azimuth, between the TRIWHEEL run and CYCLONE run.

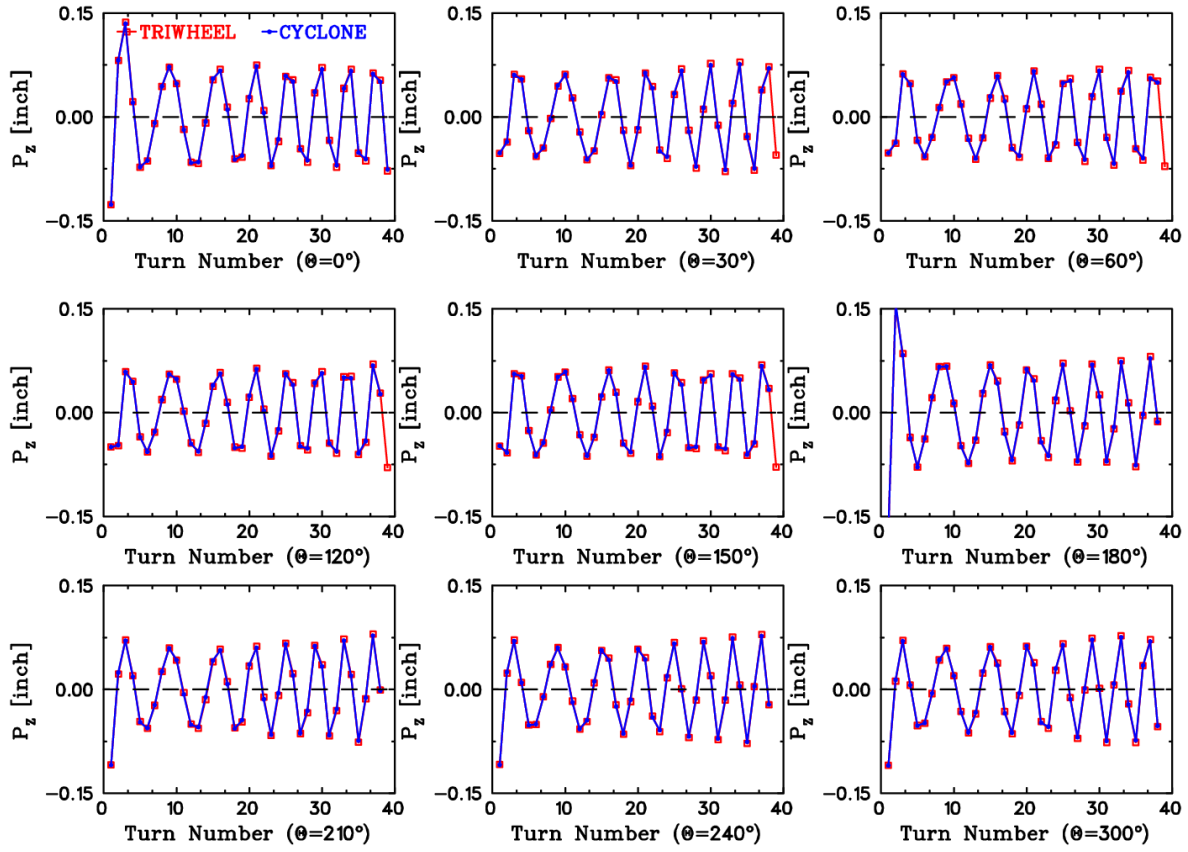


Figure 6: Comparison of single particle's axial momentum  $p_z$  recorded at various azimuth, between the TRIWHEEL run and CYCLONE run.

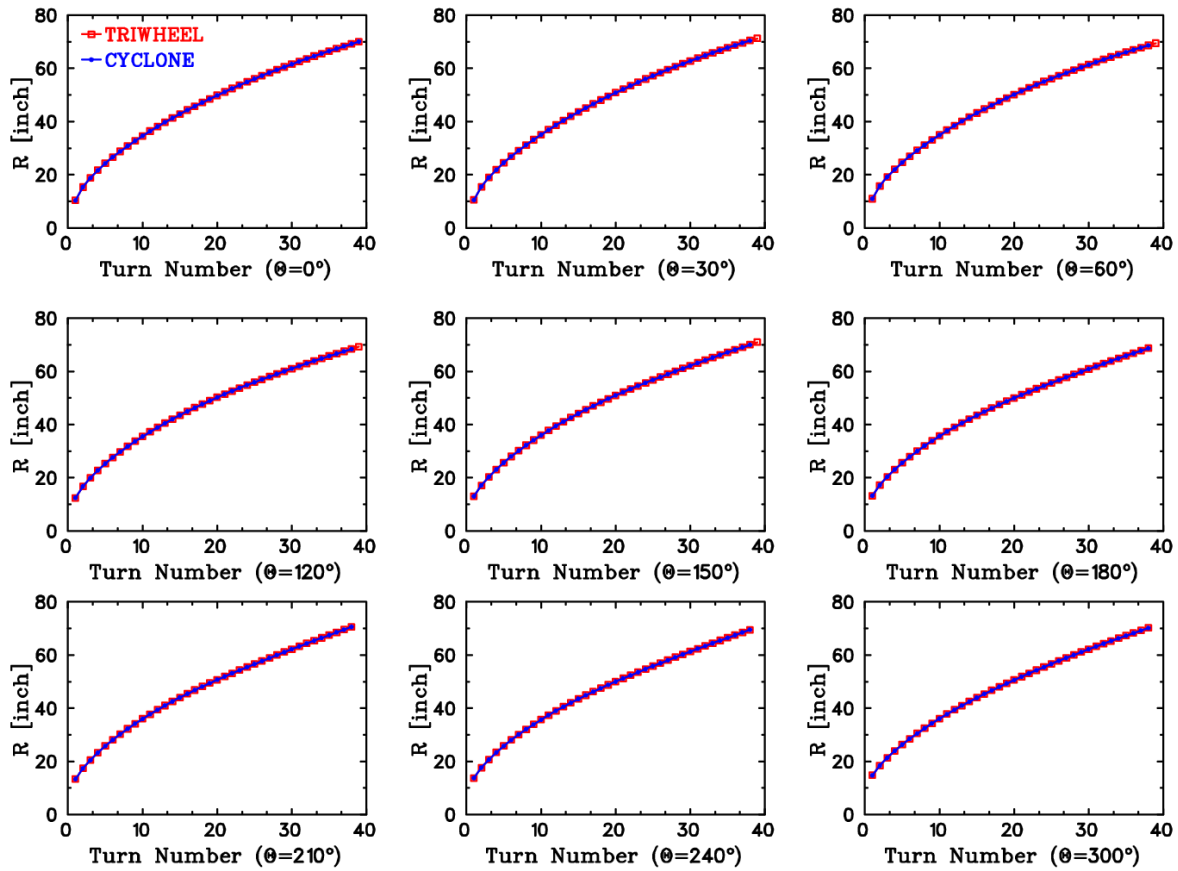


Figure 7: Comparison of single particle's radial coordinate  $r$  recorded at various azimuth, between the TRIWHEEL run and CYCLONE run.

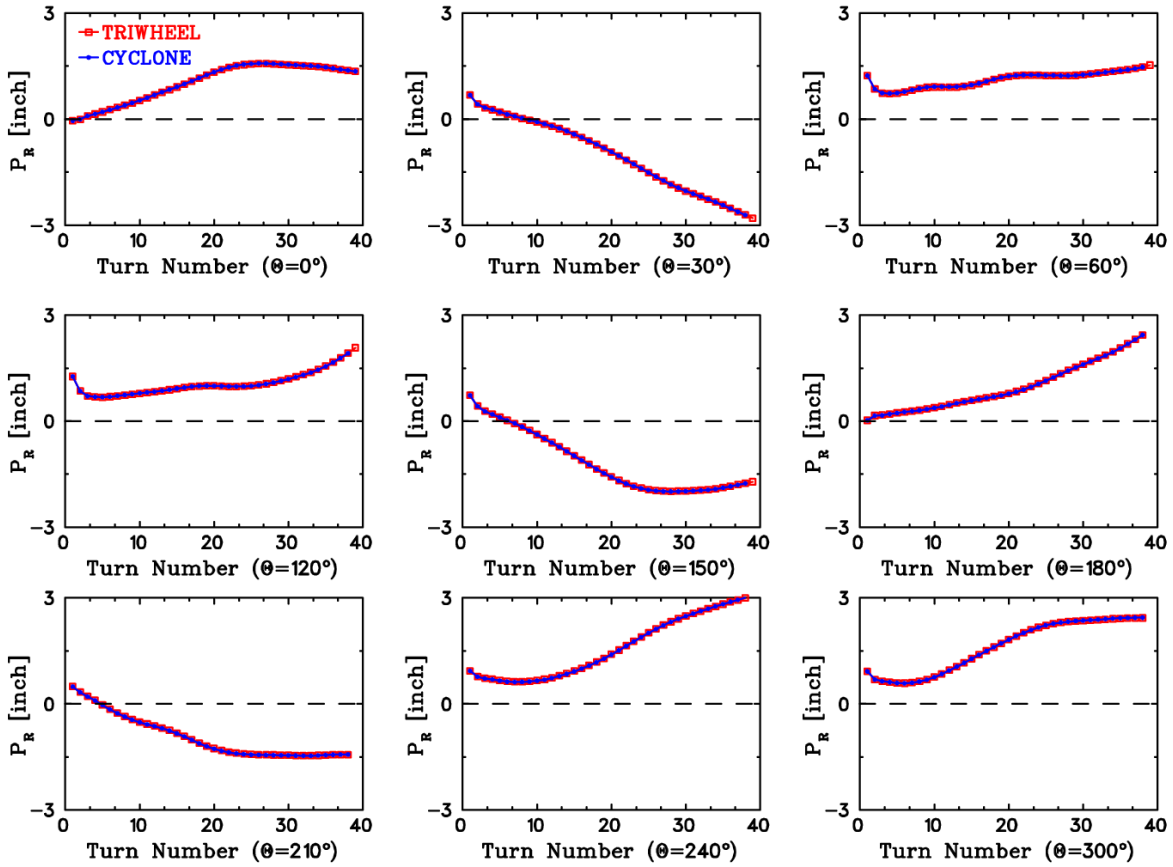


Figure 8: Comparison of single particle's radial momentum  $p_r$ , recorded at various azimuth, between the TRIWHEEL run and CYCLONE run.

## 4 Beam Characteristics

The phase acceptance of cyclotron has been an interesting topic since the early days, because it dominates the beam intensity achievable out of the machine. Fig.9 is a legacy drawing (E-338), dated back to 18 Nov. 1974, showing the 1st two-turn orbits for 5 particles of a  $50^\circ$  phase interval. We easily reproduced this result with TRIWHEEL, as shown in Fig.10. However, this picture does not necessarily mean that the machine's phase acceptance is  $50^\circ$ , because these 5 particles tracked were launched with exactly the same initial coordinates  $(x, p_x, y, p_y, z, p_z)$  at different rf time (i.e. rf phase). In other words, these particles were simply started with zero initial emittance in the transverse planes. But we wanted to establish a reasonable initial beam condition for our simulations. This drove us to revisit the injection line envelope calculation as it's involved.

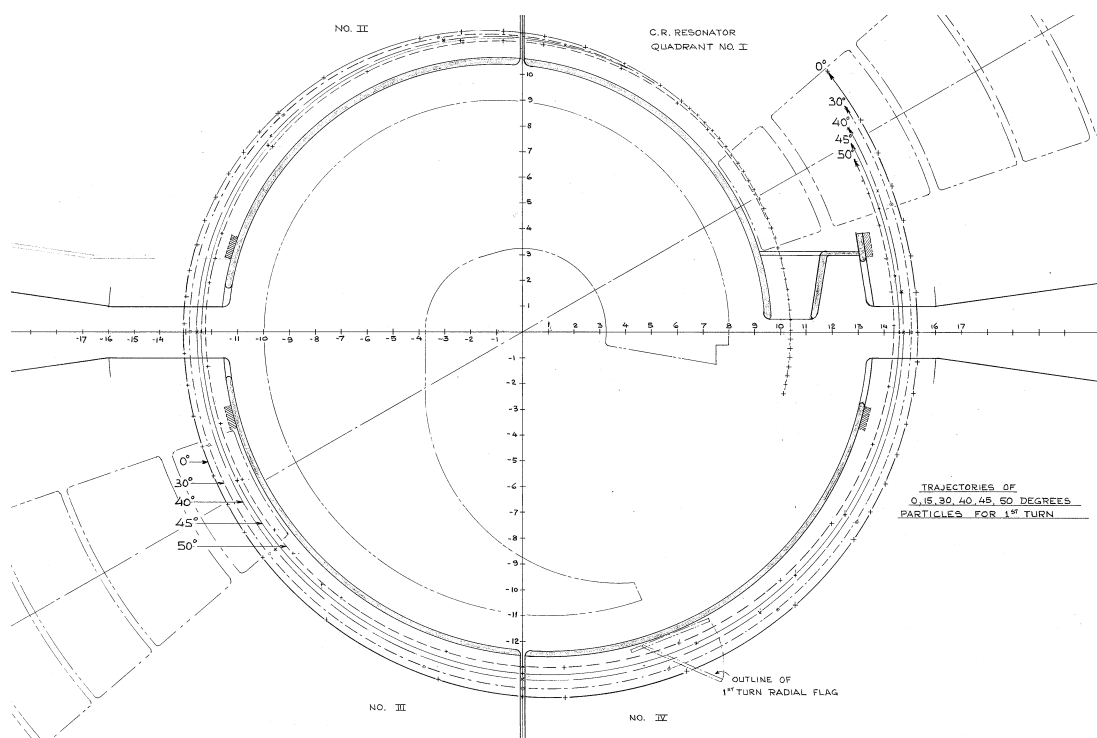


Figure 9: A legacy drawing (E-338) showing the 1st 2-turn orbits for 5 particles of a  $50^\circ$  phase interval.

### 4.1 Initial Beam

By initial beam, it's meant the condition of beam at the exit of deflector. This was calculated in the re-design of the injection line (ISIS) vertical section [6], with space charge and axial magnetic field included. In 2011, the ISIS vertical section was commissioned successfully: the theoretical tune worked right out of the box [7]. Since then, it has been running well and has achieved transmission of 70% in the cyclotron. Based on these accomplishments,

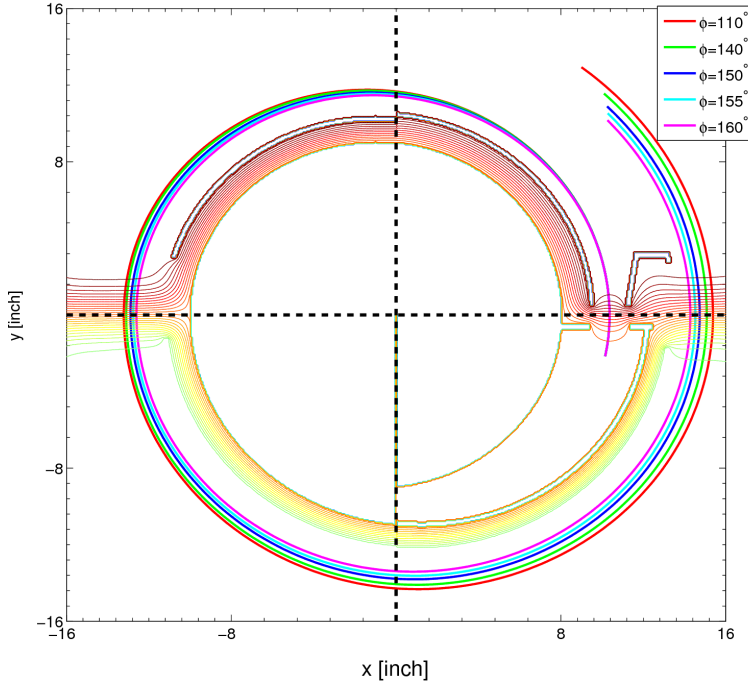


Figure 10: *Reproduced the 1st 2-turn orbits for the 5 particles of a 50° phase interval, using TRIWHEEL.*

we simply extracted the beam condition out of the envelope calculation with TRANSOPTR as illustrated in the Fig.6 and 7 of the reference [6], for bunch charge 22 pC (i.e. for a time average current 0.50 mA), for the injection phase 28°, and for the conventional deflector. This outcome is represented below as a complete 6-D sigma-matrix of beam at the exit of deflector, and displayed in Fig.11–Fig.12 in phase spaces with multi-particles.

Table 1 TRANSOPTR calculated Beam sigma-matrix at the exit of deflector

x(inch)	0.141169					
theta(rad)	0.596743E-2	0.806968				
y(inch)	0.114186	-.259220E-1	-.966584E-2			
phi(rad)	0.613146E-2	-.891379E-2	0.218187E-1	-.551112		
l(inch)	0.810058	-.235199	-.263234	-.654007	0.430760	
delta(rad)	0.931798E-3	-.319950	-.338240	-.701674	0.652538	0.958450

This is a fully coupled beam in all dimensions. It's worthy to point out that we created these particles by simply applying a fully coupled  $6 \times 6$  beam transfer matrix to the particles generated at the starting location of the vertical section where the beam was presumed to be fully uncoupled. And then, we transformed these particles from the s-based picture to a time-based picture for TRIWHEEL simulation, with the reference particle's starting coordinate given (as shown in the Fig.3).

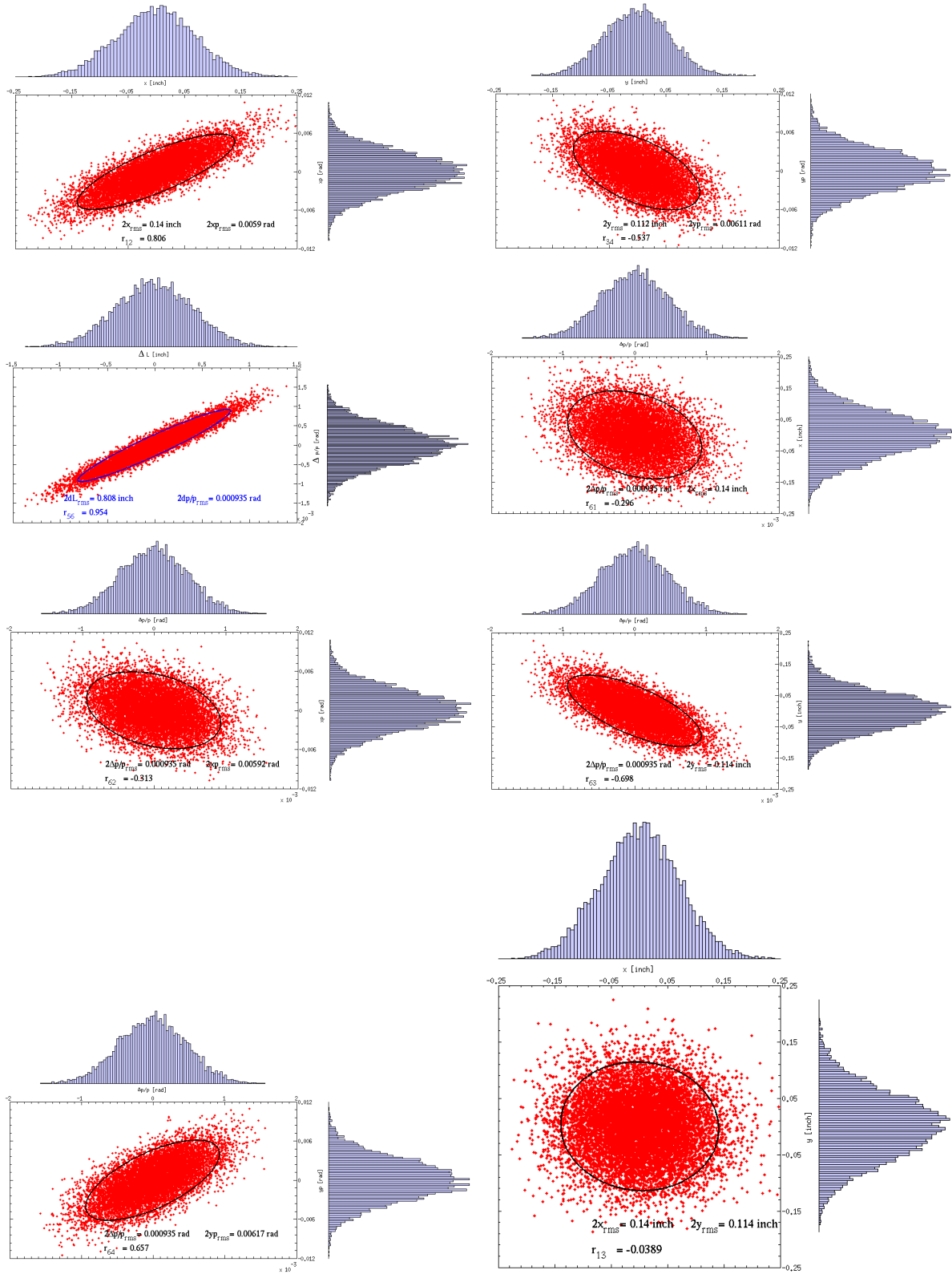


Figure 11: *Phase spaces of particles at the exit of deflector.*

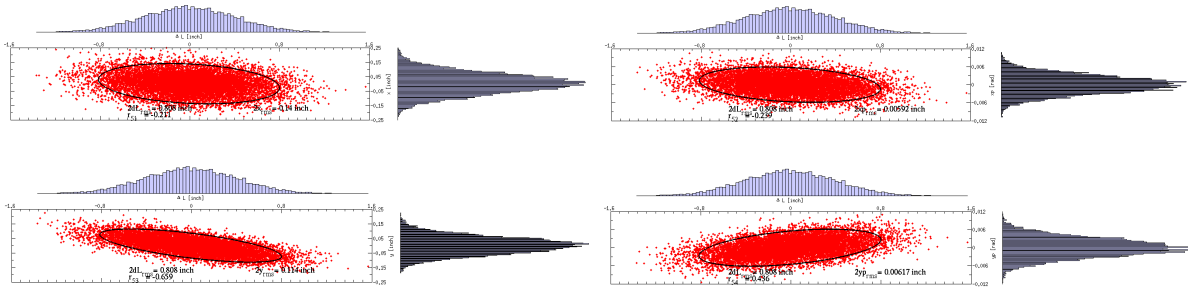


Figure 12: (Continued) Phase spaces of particles at the exit of deflector.

## 4.2 Bunch Snapshot

Fig.13 shows the resulting snapshot of bunch in the  $(x, y)$  plane, plotted once every 5 rf periods. It's seen that with the increase of turn number, the bunch stretches and the tail becomes smeared more significantly than the head. This is because the lagging particles are sitting on the falling edge of rf wave, receiving a larger gradient energy gain.

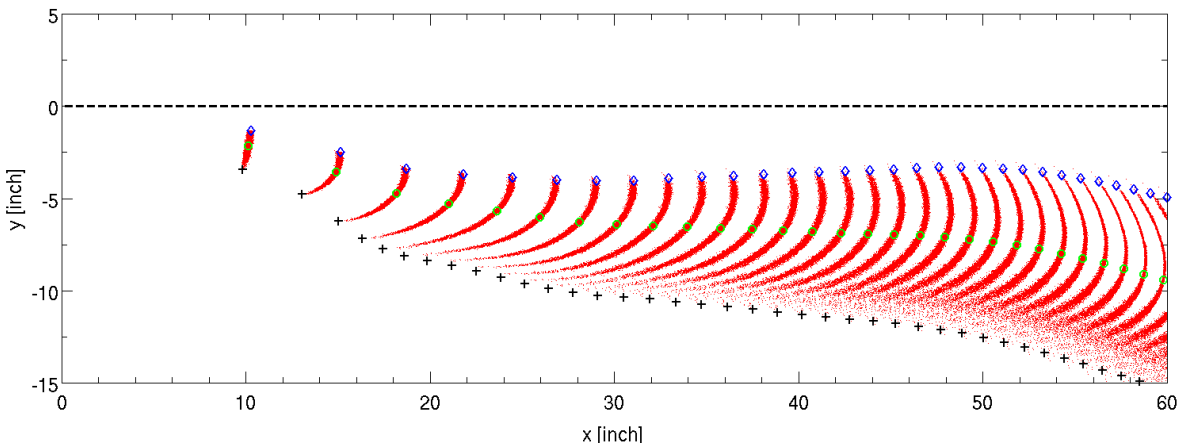


Figure 13: TRIWHEEL simulated snapshot of bunch in the  $(x, y)$  plane, plotted once every 5 rf periods (i.e. approximately once every turn). The blue, green and black signs resp. mark the leading, centered and trailing particles.

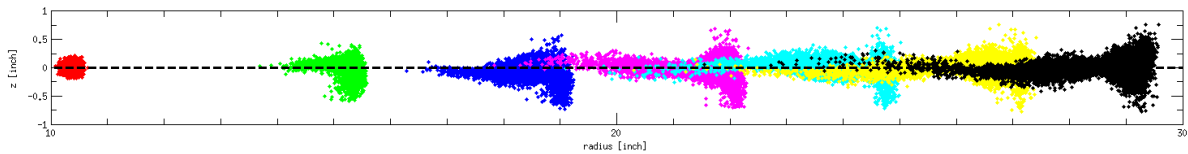


Figure 14: Snapshot of bunch in the  $(r, z)$  plane, plotted once every 5 rf periods (i.e. approximately once every turn). Here we only plot the first 6 turns.

Fig.14 shows the snapshot of bunch in the  $(r, z)$  plane over the 1st 6 turns. The sharp radial edge corresponds to those particles sitting on the crest of rf wave. The particles near the crest undergo weaker vertical focusing, that's why they emerge with larger vertical oscillations; while the particles far from the crest receive less energy gain, that's why they fall more inboard radially.

With the increase of energy, the radius gain due to energy gain is decreasing while the bunch's tail is lengthening. As an example, Fig.15 shows the radial density distribution of particles on individual turns at azimuth of LE2 probe. Adding up all these distributions gives the LE (Low Energy probe) scan. This is shown in Fig.16, which appears to be similar to the result measured with a short bunch (see Fig.5 in reference [8] but note that in this plot the 1st turn is missing.).

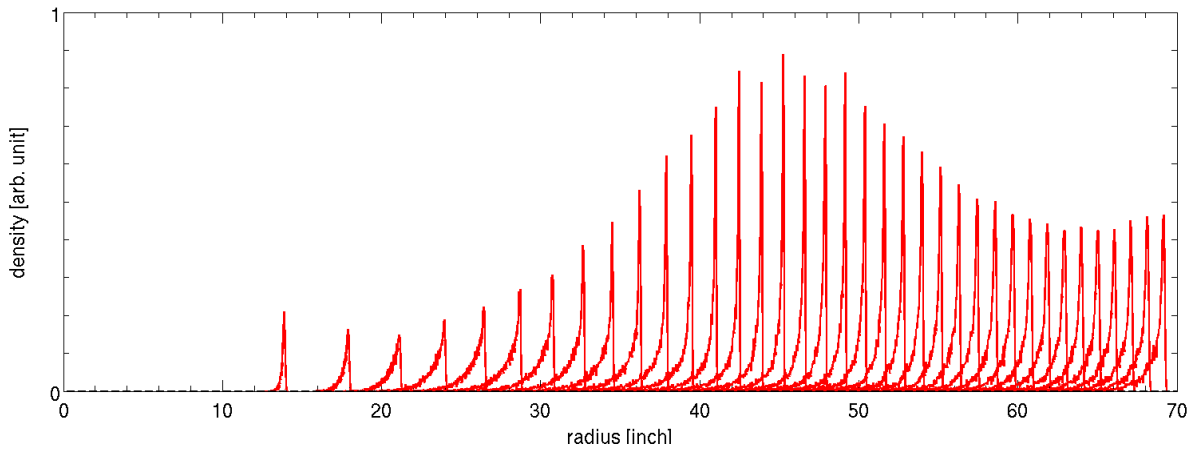


Figure 15: *Radial density distribution of particles on individual turns at azimuth of LE2 probe.*

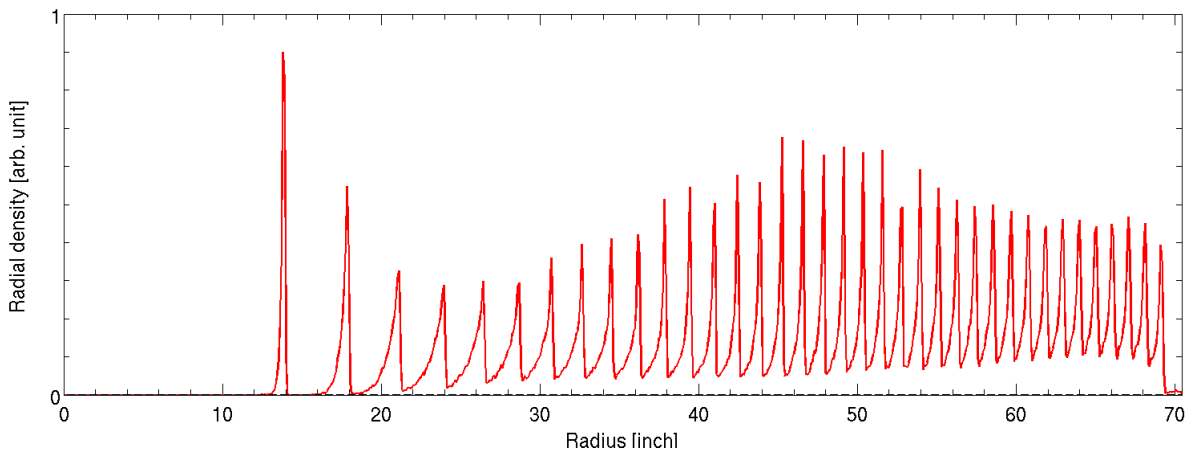


Figure 16: *Simulated LE scan, showing the turn pattern at azimuth of LE2 probe.*

### 4.3 Phase Acceptance

In the first a few turns, the vertical focusing that particles experience is dominated by the electric rather than the magnetic focusing. Thus, the phase acceptance is determined by two factors: the leading particles must undergo enough vertical focusing to survive from a vertical aperture, while the trailing particles must receive enough energy gain to get around the centre post. Fig.17 shows the phase dependent vertical focal power of par-axial particles when they pass through the first 2 gaps (injection gap plus the following dee gap). Fig.18 shows the good particles which were accelerated to high energy, as well as the bad particles which were lost either vertically or vertically. This indicates that the machine's phase acceptance reaches  $\sim 60^\circ$  when space charge force is not taken into account. This is consistent with the measured result [9].

Alongside, Fig.19 shows the good particles rf phase interval vs. turn at RHS dee gap centre-line crossing. Apparently, the phase interval is moved from preceding to lagging phases during the first 10 turns and then back to zero. This is resulted from the effect of a magnetic field bump in the centre region (see the legacy file "policyinita6.dat"). It's also noticed that the phase interval gradually reduces to  $\sim 45^\circ$  after about 30 turns. This is probably arisen from a phase bunching effect due to magnetic and electric configurations.

The bad particles were mostly the leading ones; they got lost over the first 10 turns in the vertical plane. This is shown in Fig.20 and Fig.21 both.

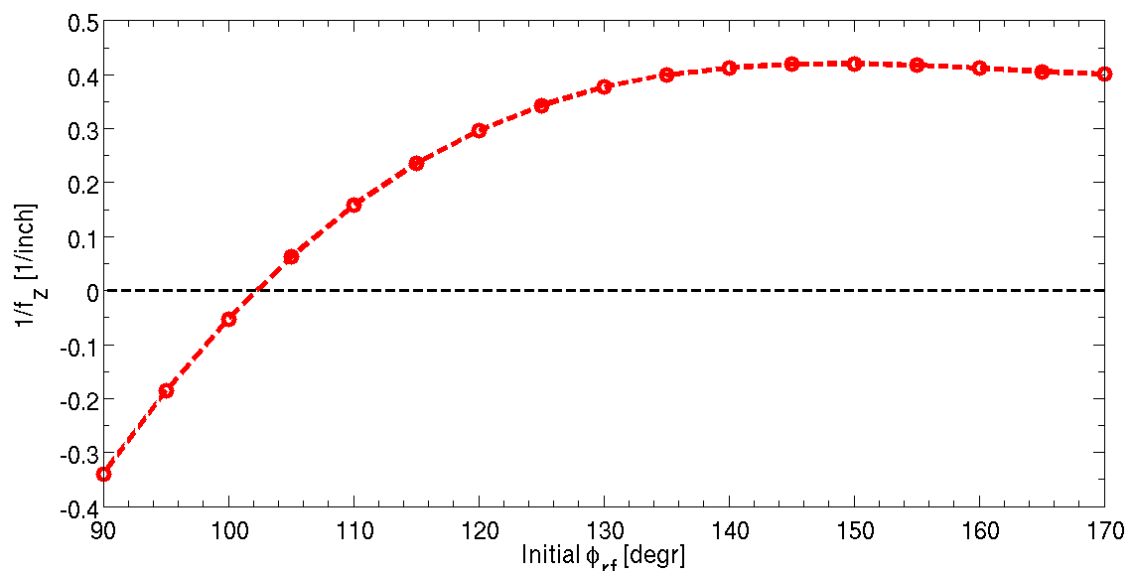


Figure 17: TRIWHEEL calculated vertical focal power vs. the initial rf phase of par-axial particles when they pass through the injection gap plus the following dee gap.

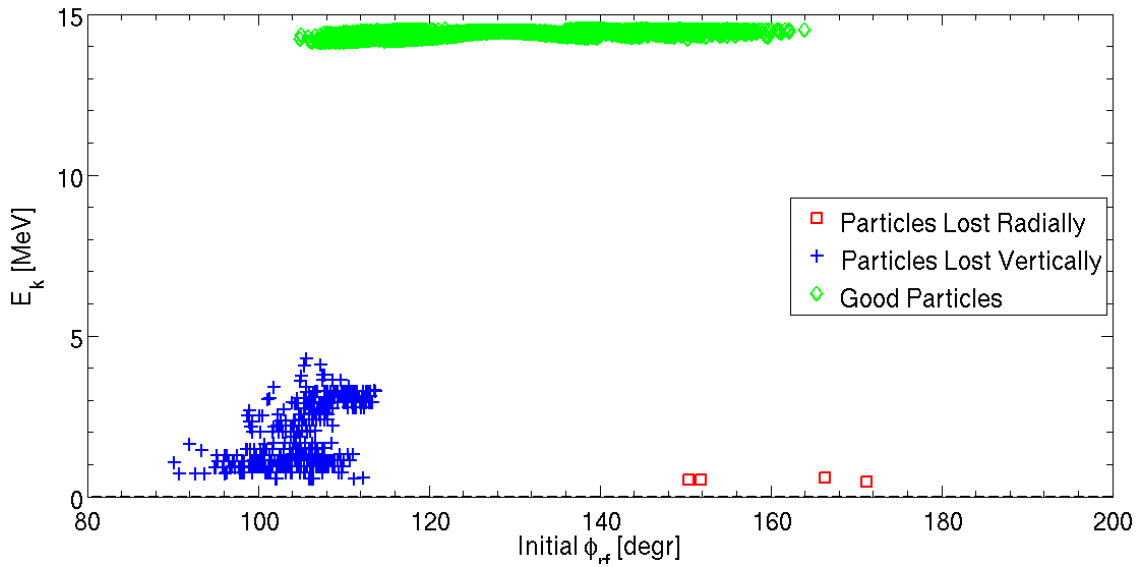


Figure 18: TRIWHEEL simulated good particles (Green) and bad particles (Red and Blue). The good particles were all accelerated to high energy (here only plotted up to 14 MeV), while the bad ones were all lost either radially or vertically. This indicates that the machine's phase acceptance reaches about  $60^\circ$  (when space charge force is not taken into account).

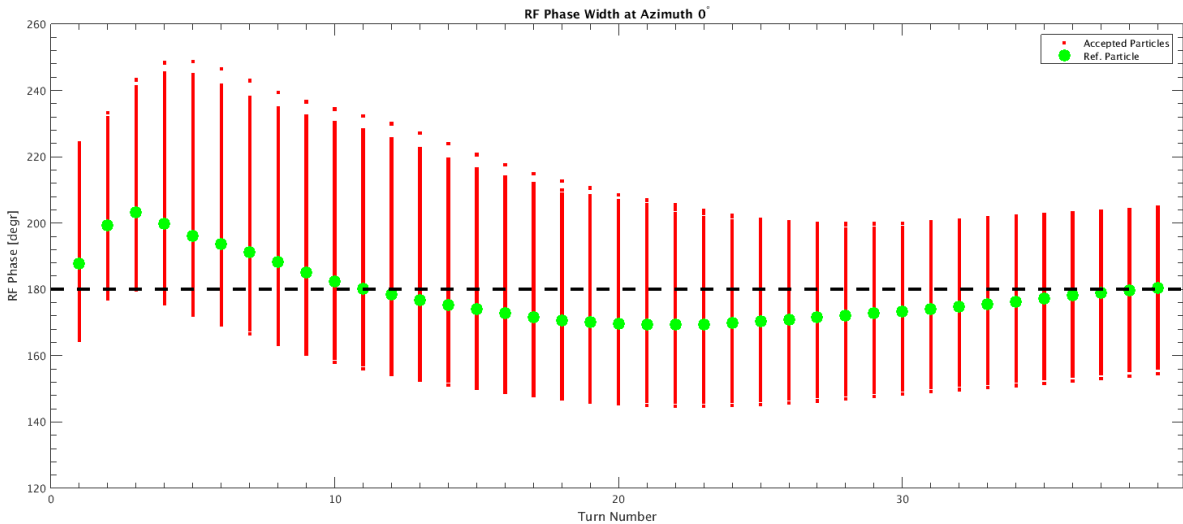


Figure 19: The good particles rf phase width vs. turn, at RHS dee gap centre-line crossing. It's seen that the phase interval is moved from preceding to lagging phases during the 1st 10 turns and then back to zero; also noticed that the phase width gradually reduces from  $\sim 60^\circ$  to  $\sim 45^\circ$  after about 30 turns.

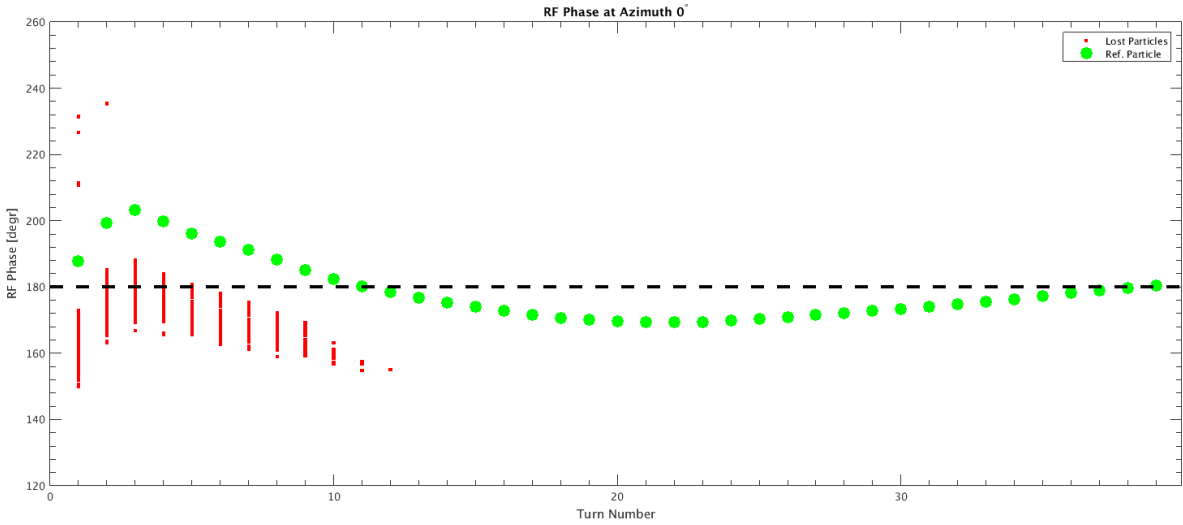


Figure 20: *The bad particles rf phase (Red) vs. turn, at RHS dee gap centre-line crossing. It's seen that these particles are mostly the leading ones and they get lost over the first 10 turns.*

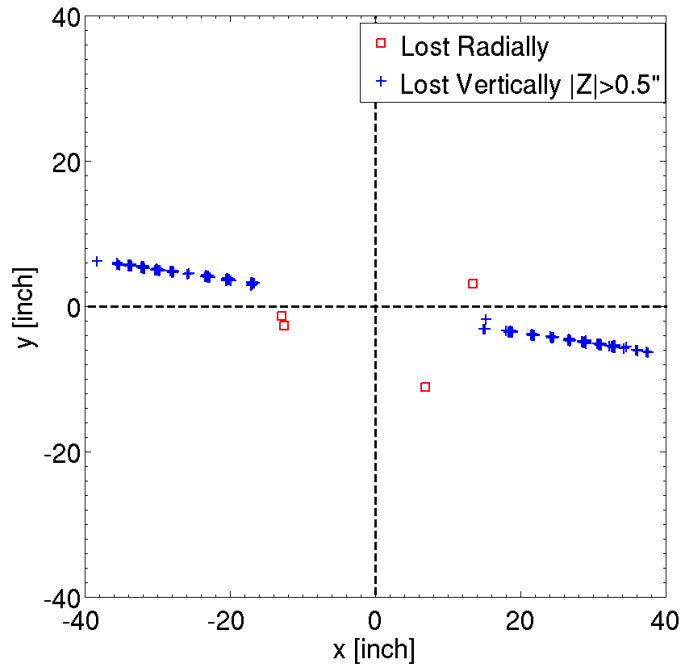


Figure 21: *The lost particles distribution, showing that most losses occur in the vertical aperture which extends radially on opposite dee segments.*

## 5 Conclusion

We improved the centre region model of TRIUMF cyclotron by using the realistic electrode geometries and the recalculated 3-D electric field map, plus the refined initial beam condition. The simulation gives correct picture of beam snapshot in each plane. The simulated LE scan and machine phase acceptance appear to be consistent with the measured results. This improved model shall form the basis of further studies on the centre region with space charge force taken into consideration.

## 6 Acknowledgment

The helpful discussions with R. Baartman and F.W. Jones about the initial beam are appreciated.

## References

- [1] T. Planche, R. Baartman, Y. Bylinsky, Y.-N. Rao, *SPACE-CHARGE SIMULATION OF TRIUMF 500 MEV CYCLOTRON*, Proc. 21st Int. Conf. on Cyclotrons and their Applications, (2016)
- [2] G. Dutto, C. Kost, G.H. Mackenzie, M.K. Craddock, *OPTIMIZATION OF THE PHASE ACCEPTANCE OF THE TRIUMF CYCLOTRON*, AIP Conf. Proc. 9, 340 (9172).
- [3] G. Dutto, M.K. Craddock, *FOCUSING IN RF ACCELERATING GAPS WITH ASYMMETRICALLY CURVED ELECTRIC EQUIPOTENTIALS*, Proc. 7th Int. Conf. on Cyclotrons and their Applications, 271 (1975).
- [4] C.J. Kost and F.W. Jones, *RELAX3D User's Guide and Reference Manual*, TRI-CD-88-01, V3.0, January 1992.
- [5] Y.-N. Rao, *Maintenance and Usage of Computer Program CYCLONE for TRIUMF Cyclotron*, TRI-DN-02-27, Dec.19, 2002.
- [6] R. Baartman, *Optics design of the ISIS Vertical Section Replacement*, TRI-DN-09-11, September, 2009.
- [7] R. Baartman, *Designing the 300 keV Vertical Injection Line*, September 24, 2013.
- [8] T. Planche, Y.-N. Rao, R. Baartman, *MEASUREMENT OF TURN STRUCTURE IN THE CENTRAL REGION OF TRIUMF CYCLOTRON*, Proceedings of Cyclotrons2013, Vancouver, BC, Canada.
- [9] L. Root, *Dec 2, 2009 Development Shift Summary*, 2009.